HIGH IMPEDANCE FAULT LOCATION IDENTIFICATION USING BAYESIAN ANALYSIS IN A SHIPBOARD POWER SYSTEM

by

JOSEPH DIEKER

B.S., Kansas State University, 2010

A THESIS

submitted in partial fulfillment of the requirements for the degree

MASTER OF SCIENCE

Department of Electrical and Computer Engineering
College of Engineering

KANSAS STATE UNIVERSITY
Manhattan, Kansas

2012

Approved by:

Co-Major Professor
Dr. Sanjoy Das

Approved by:

Co-Major Professor
Dr. Noel Schulz

Abstract

In a shipboard power system (SPS) there are many possible locations for faults along power lines. It is important to identify the location and isolate these faults in order to protect the equipment and loads. The shipboard systems represented in this research are based on an all-electric ship that is presented by Corzine and a simplified version of the same ship. This research considers faults at the ends on the lines. Sensors collect data in order to determine where the fault has occurred. The fault location identification algorithm being presented uses data collected from simulations of different switch configurations and different loads. After the data is collected, Bayesian techniques are used to determine where the fault is located. An online training technique is presented to adjust to changes in loads over time to increase the accuracy of the algorithm.

Table of Contents

List of Figures

List of Tables

Acknowledgements

I would like to thank my academic advisors, Dr. Noel Schulz and Dr. Sanjoy Das, for the guidance and support on the path of completing my Master's program. I would also like to thank the other committee members, Dr. Caterina Scoglio and Dr. Bala Natarajan, for their guidance.

I would like to give thanks to the United States Office of Naval Research for their financial support through grant N00014-10-1-0431 under the DEPSCoR program.

Finally, I would like to thank my family and friends for their encouragements and support throughout this program and before to get to this point. A special thanks to my Mother for her help in editing this thesis.

Chapter 1 - Introduction

Electrical power has become one of the main necessities in the modern world today. A fault along that system, that could cause outages and damage, is one of the main problems in the system. It is important that the fault is located in the system so that it can be isolated. If the fault is not isolated, electrical equipment and other parts of the system could be damaged for the long term.

1.1 Fault Detection and Location

Fault detection is a prerequisite for outage management in a shipboard power system. Outages on a power system cannot be fixed without the location of the fault. Grounded faults can cause major outages because of the effect on the power electronics that control the voltage and current [1]. There are various types of fault detection and location schemes or processes out there for alternating current (AC) and direct current (DC) power systems.

In AC voltage power systems the fault can be located using many methods. The voltage and current measurements at local ends of transmission lines can be used to determine the location of the fault [2]. Phase measurement units can be used to determine the fault location along complex distribution systems [3]. Transients in measurements can be used in fault detection schemes [4]. Finally, tracing superimposed signals along the medium voltage railways can be used to find a fault [5]. Complex AC systems have plenty of parameters that can be used as is shown above, to find faults along a system. The main parameters that change during a fault include voltage and current magnitude and phase angle.

There are many types of DC voltage power systems high voltage direct current (HVDC) power systems and medium voltage direct current (MVDC) systems. Less research work has been done to determine faults in these systems. This research work presents a MVDC shipboard power system. DC systems, as compared to AC power systems, have a minimal amount of parameters to consider when faults occur. These parameters include voltage and current magnitude.

1.2 Shipboard Power System

The shipboard power system is the focus of this research. The U.S. Navy is looking at the next generation ship, which may include a DC power system that includes multiple power elements. These power elements include multiple generators, power lines or buses, and loads. The generators throughout the system generate AC power. This AC power is then converted to DC by three-level bridge converter. A voltage controller and current controller run this converter in order to keep the DC voltage at the required level.

There are many situations that can cause a fault on a shipboard. These situations include being hit be artillery from enemy ships and daily wear and tear in the shipboard system. However, especially in naval battleships it is important to locate and isolate a fault so that further actions that need power, such as retreating or firing a rail gun, can be taken [6]. Some of the current techniques for locating faults are reviewed in Chapter 2.

1.3 High Impedance Faults

The faults that are the hardest to locate are higher impedance faults that have less effect on the overall system. In this research, DC shipboard power systems are simulated with high impedance faults. Lower impedance faults are assumed to be found and isolated swiftly with

protection equipment before the high impedance fault location algorithm is required to locate the fault. Each simulation includes different configurations and load distributions. A method is introduced to correctly identify high impedance fault locations along power lines. This method is rigorously tested in order to justify choices. Additionally the described method is introduced to adapt to changes in the load during operation of the system.

1.4 Thesis Objective

The objective of this thesis is to develop a novel way to determine the location of high impedance faults in a shipboard power system. In order to collect fault data, shipboard power systems needs to be modeled and simulated. Each part of the system, generator, converter, power line, and load, need to be modeled in the selected simulation software. A method must be produced to accurately locate high impedance faults in the system. Bayesian methods are used to determine the location of the faults in the power system. The sensor currents, during the fault, are used as the input to the algorithm. Maximum a Posteriori and maximum likelihood estimates are then used to determine the fault location parameter. These methods should be able to adapt to normal changes in the load distribution and topology. An online method is proposed in this thesis to become more accurate during these load shifts. Test cases, such as random fault impedances and multiple locations, are used to fully test these methods throughout the process.

Chapter 2 - Review of Related Works

The importance of fault detection and location in any system was discussed in the previous chapter. Various fault detection and location algorithms have been developed over the years. The following Chapter discusses the methods presented recently.

2.1 Fault Detection

One of the ways to detect and locate faults includes measurements at the rectifier and converter ends of the power system as presented by Nanayakkara [7]. The algorithm takes as inputs the arrival times of the fault current effect at the ends. This method considers a simplified system with AC Systems on each end of a there line segments in series. When this system is compared to the proposed shipboard power systems, the line segments are longer in the terrestrial systems, which causes the time delay to the ends to determine the fault location. The implementation would also be more complex when adapting to the many line segment and intermittent loads in the system presented.

In [8], a handshaking method is implemented to detect and isolate faults using AC circuit breakers behind DC converters along the system. Handshaking is a process of negotiation between different entities until they come to a consensus. This consensus in this case is the fault location in the power system. AC circuit breakers are placed intermittently in a DC system behind converters. Since DC breakers are more expensive, this paper proposes a more costly method with a multi-terminal system. The method used is a handshaking method between the breakers to use DC switches, faster than DC breakers, to isolate a fault.

However, the fault could cause many problems to the power system protection equipment and loads over time [9] [10]. There are many techniques that have been developed to find high

impedance faults on power systems, including wavelet-based algorithms [11] and multi-layered perceptron neural networks [12]. The first method proposed, wavelet-based algorithm, is implemented for AC power systems and not adaptable to the DC shipboard power system. Multi-layered perceptron neural networks accuracy falls when used in a more complex system like that used in this research. Noise pattern analysis was not applicable in the system proposed because of the architecture of the shipboard system.

Another paper [13], suggests using noise pattern recognition to locate faults in an ungrounded DC power system. The method uses pattern recognition of high-frequency noise due to switching events of converters. The noise patterns are recorded using phasor measurement units (PMUs) in order to record dynamic characteristics in terms of derivatives. The main drawback of this approach is the cost of PMUs.

2.2 Shipboard Power System Detection

In [14], Kusic extends state estimation for AC shipboard power systems to fault detection. Sampled real time current and voltage data is collected and synchronized to estimate the state. Using magnitudes and phase angles at the buses and transmission lines the location of the fault can be found with accuracy. This paper goes into replacing missing data using nearby measurements to estimate the missing data.

A technique to determine the fault location using active impedance estimation is presented by Christopher [15]. In the paper, a short current spike is injected into the system and the voltage and current transients are recorded. These responses can then be used to the equivalent system impedance. Since the loads in a shipboard power system are usually much larger than the bus impedances, the fault impedance usually dominates the impedance estimation.

However, with increase in impedance of the fault the ability to find the fault with this method becomes less accurate.

Another type of fault, usually bypassed by most protection methods, is an intermittent fault. Intermittent faults cause short duration transients in the power system. These faults are the most elusive and expensive faults to detect and locate. The method, provided in [16], injects a modulated signal at one location in a system. Then, comparing the signal at another location on the power system provides the fault diagnosis.

Some of the more novel ways of fault location is the method produced in [17], [18] and [19]. Reference [17] proposes the use of artificial neural networks to determine the location of the faults on the shipboard system. Transient properties of current and voltage signals are used as the input to determine the location of the fault in the system. Machine learning techniques are used to diagnose and locate faults in a shipboard power system in [18]. Finally, a genetic algorithm is proposed to determine the location of the fault in the power system [19]. Most of these estimations use their methods to find grounded faults. However, most have some concern when it comes to high impedance faults.

Pan [20] describes an approach to finding high impedance faults in a shipboard power system. Much like [21], the paper proposes a novel way of noise pattern analysis. Repetitive switching in the conversion gear when a fault occurs causes the noise in the current signal. However, when later analyzing the proposed model for this thesis in the simulation, the noise patterns found in this paper are not found in the signals. The signals are not found because the model in the paper has more protection equipment than the models proposed in this thesis.

2.3 Bayesian Fault Detection

Bayesian methods are proposed for use in diagnosing and locating faults in an AC voltage power system in multiple papers [22-24]. These papers use previous data in order to compute the expected values of situations in the system. These situations include faults along the system as well as normal conditions. This is then compared to the computed results in order to predict the fault location in the power system. The advantage of using the Bayesian networks is that the method adjusts the parameters continuously. This allows for adaption to changes in the natural state of the system, such as load changes and switching topologies. This thesis adapts these methods to the DC power system in order to find faults in the shipboard power system.

2.4 Summary

Many techniques have been developed for fault detection in power systems. However, there is a lack of development in fault detection for DC shipboard power systems. This is especially true with regards to high impedance faults on a power system. This thesis will look for a novel method to determine the high impedance fault location on a MVDC shipboard power system.

Chapter 3 - Models of the Shipboard Power System

In this research, two shipboard power systems (SPS) models are presented. These models were provided by the United States Office of Naval Research for this work. The first is a simple model useful in formation and implementation of new, knowledgeable concepts. The second model is more complex and implemented to test those theories as a more realistic representation of the shipboard system. The systems are simulated in MATLAB Simulink using the SimPowerSystems toolbox.

MATLAB is a numerical computing package that includes its own programing language. It was developed for the ease of use in numerical computing, including matrix calculations and plotting of data. It allows interfacing between itself and other programs written in different languages. MATLAB also includes an extension, Simulink, for graphical interface simulations. A toolbox that is included in Simulink, SimPowerSystems, allows the simulation of power equipment in the MATLAB environment. This toolbox is used to simulate the power system in this work.

3.1 Simplified Model of the Shipboard Power System

The simple model of the shipboard system contains two generators, four load zones and two buses as presented in [25]. The generators, as shown in Figure 3.1 below, are located at both ends of the system. Each generator provides power to both buses in the shipboard power system. The main generator, shown on the right, operates at 8 MW and the distributed generator produces 6 MW [25].

Figure 3.1 Simplified Model of a Shipboard Power System [25]

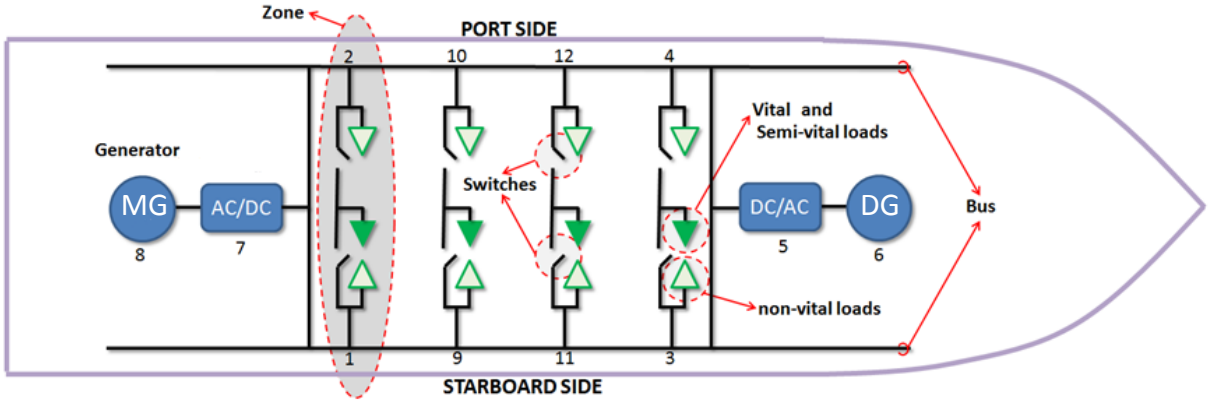

The generators are connected to the loads using two buses. These two buses are made up of power lines. There are two different varieties of power lines that appear in the SPS, one that connects the generators to the buses and another between the loads. These lines differ based upon the resistance of the lines. The value of resistance between the generator and buses is $1.85*10^{-3}$ Ω. The power lines between the loads have $1.85*10^{-4}$ Ω of resistance [25].

The loads in the system represent motors, artillery and other equipment in the ship. There are four load zones in the model. Each load zone is connected to both buses. The load zones include three types of loads: vital, semi-vital, and non-vital. These priorities are added so that if a fault occurs, loads with higher priority can be given preferential treatment. The vital loads would include motors and artillery. Lower priority loads could include computer equipment, communication equipment, and personal use loads. In each load zone there are two non-vital loads, one connected to each bus, which consumes 0.5 MW [25]. Two switches connect the semi-vital and vital loads to each bus. The switches are considered to be mutually exclusive: meaning either connects the loads to the starboard or port side bus. The values of the semi-vital

and vital loads are 1 MW and 0.5 MW, respectively [25]. The loads are represented as purely resistive and based on the AC/DC rectifiers keeping the voltage level constant.

3.2 Corzine Model of the Shipboard Power System

The second model, presented by Corzine, adds more complexity to the model [26]. It adds two more generators, a main generator and distributed generator. The total number of generators equals four now, with the two distributed generators producing 4 MW and the two main generators operating at 6 MW [26].

This model has five load zones that, as before, contain two non-vital loads, one semi-vital load, and one vital load. There are switches that connect the higher priority loads to either the starboard or port side bus. There are also two new load zones added between a generator and a bus, as seen below in Figure 3.2. These two new loads are inserted into the model to represent the motors of the SPS. The motors are represented single vital load and are connected to one bus and a generator through switches. The power dissipated by each of the load priorities are the same as the previously presented load.

Figure 3.2 Simplified Model of a Shipboard Power System (adapted from [26])

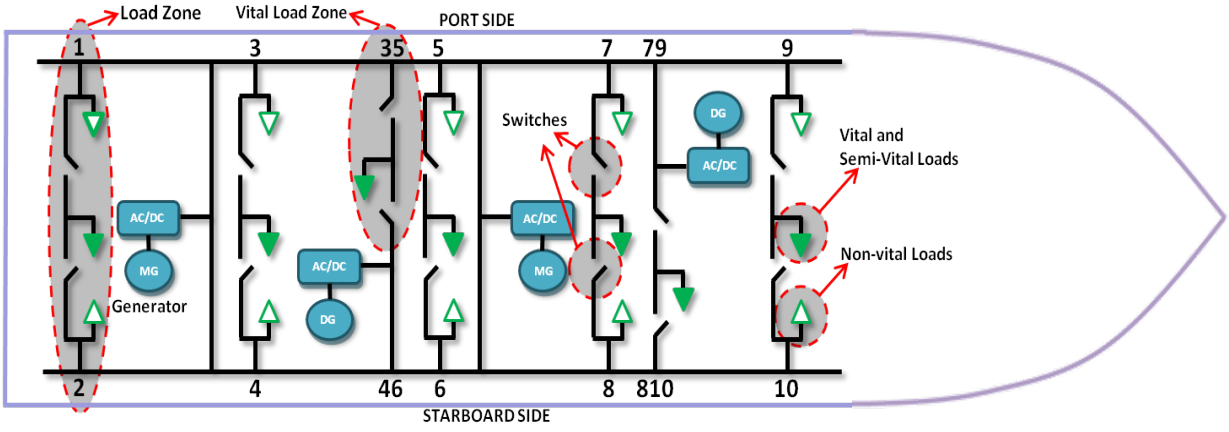

3.2 Simulation of the Power Systems

MATLAB Simulink was chosen to simulate the two models presented by this research. The power electronics were simulated using the SimPowerSystems toolbox. This could allow for future use with real time simulators, such as OPAL-RT.

3.2.1 Simulations of Generator and AC to Controlled DC Converter

The generator and AC/DC converter are all integrated into one subsystem in the simulation, shown below in Figure 3.3. In the Figure, the power system elements are colored blue with black outlines and the control system is in yellow. A simplified synchronous machine model is used to simulate the mechanical power produced. The default parameters are used except for the nominal power and the voltage. After the machine, a filter is attached to clean up the noise that may be caused from the power electronics or loads down the line. A transformer is then added to step down the voltage to the needed voltage. Another filter is added in the lines again after the transformer.

Figure 3.3 Generator and AC to Controlled DC Converter in Simulink

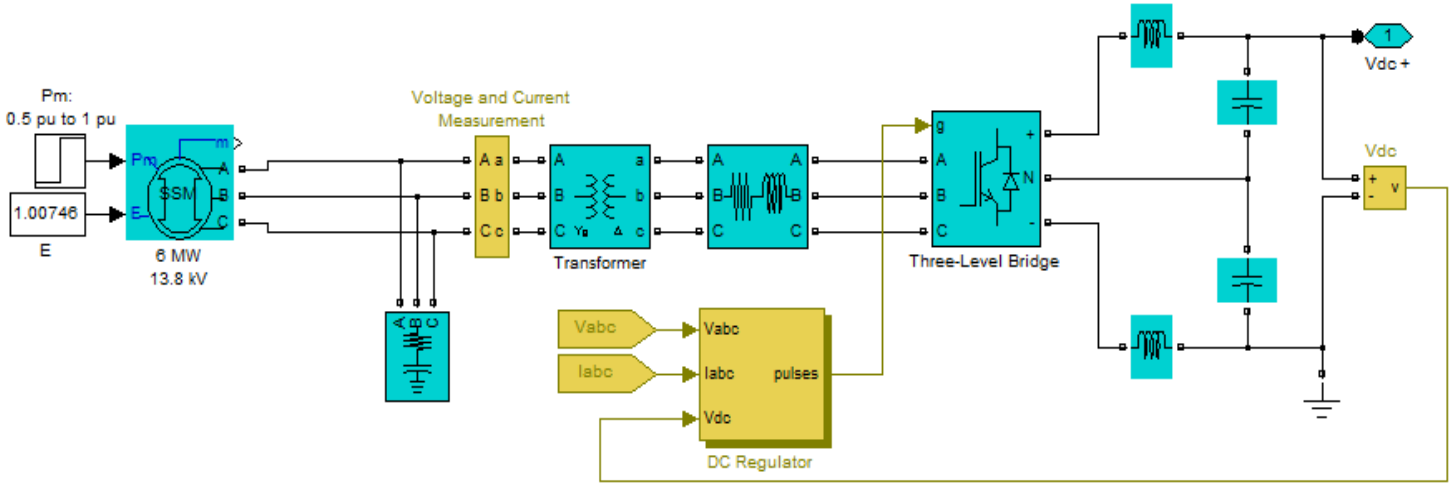

The AC/DC converter has three main parts: a controller, a three-level bridge and filters. A current regulator and a voltage regulator control the three level bridges. The controller keeps the voltage after the bridge at 4.15 kV. The filter after the bridge cleans up the voltage so that it will stay within ±5% of the previously stated value.

3.2.2 Simulations of Loads in the Shipboard Power System

The loads in the system, as stated above, are represented as purely resistive. This is a simplification of a load that probably contains an AC load and an AC to DC converter to connect the load to the DC bus. The loads are constant resistances based on the assumption that the controlled DC voltage stays at the per unit level. The loads are shown below in Figure 3.4, as before the control signals are in yellow and the power system is in blue. Ideal switches are used to connect the vital and semi-vital loads to the two buses. The logical operator is used to help simplify the simulation so that one signal is only needed to control the switches. This also prevents the high priority loads from connecting to both buses and prevents a loop in the SPS.

Figure 3.3 Load Zones Represented in Simulink

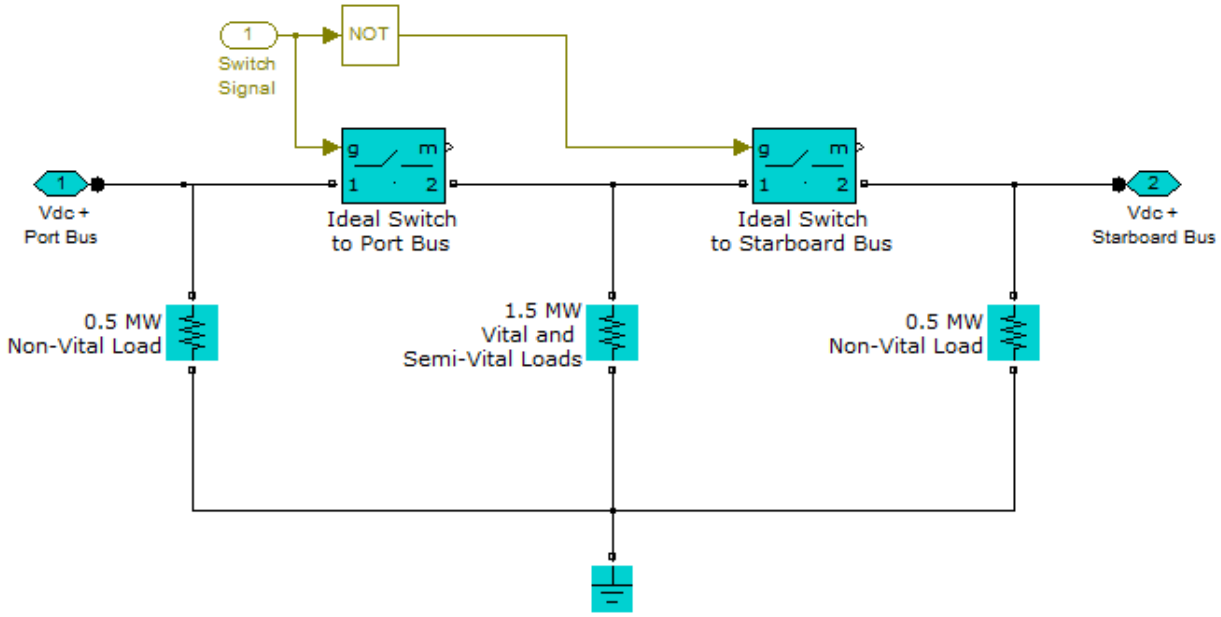

3.2.3 Simulations of Power Lines in the Shipboard Power System

The power lines have three main components in this model: the resistance of the power lines, the current sensors at the ends of the lines, and the faults at the end of the lines. The faults are connected to the line using switches that are controlled by a signal that can be changed during the simulations. The power line model is shown below in Figure 3.4.

Figure 3.4 Load Zones Represented in Simulink

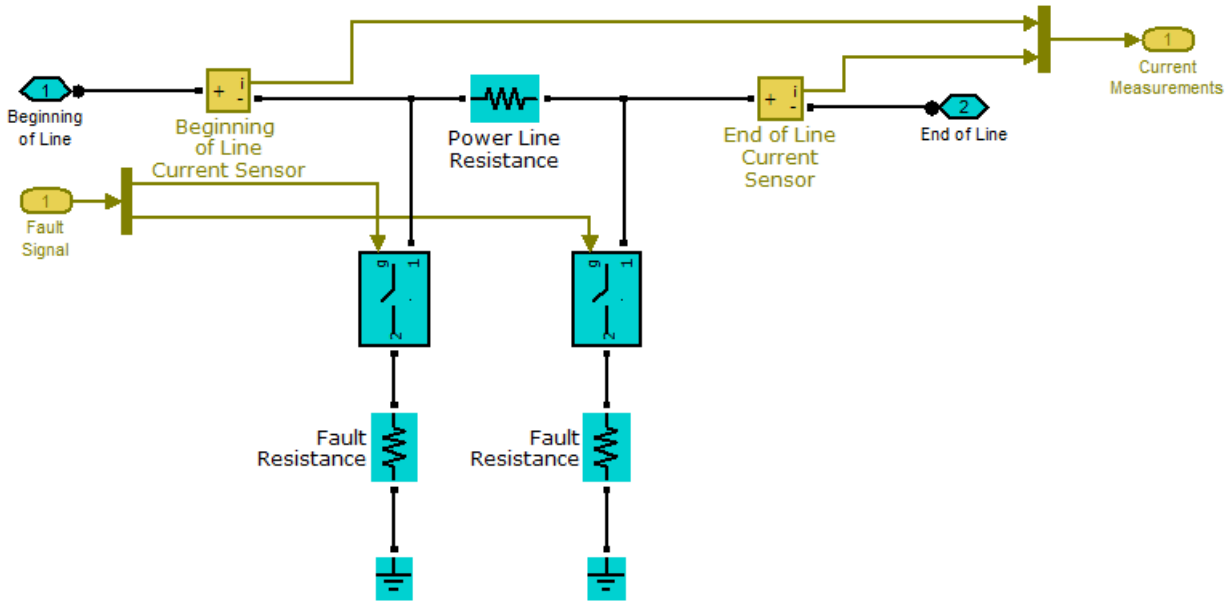

The fault impedance is a key aspect in this research. In order to determine the impedance range for testing, simulations are run to determine which impedances affect the system and can be easily found. The other end of the spectrum, simulations are run to determine how high the impedance can be increased in order to determine when the fault has no visual effect on the current levels. The range of impedance that is high enough to no longer affect the power electronics and still affect the current levels is 100*R to 1000*R. The R in this range is the power line resistance.

3.3 Current Data and Sensor Collection

After all the models have been developed, it is time to collect and analyze the data. The goal of this analysis is to determine if there is an easy way to determine the location of the fault.

3.3.1 Sensor Location on the Power Systems

The sensor placement is important to the correct identification of a fault location. The placements that were chosen in this project were at the ends of the lines. Since the fault locations are on the transmission lines, this seems like a logical placement. The placements on both the Corzine and Simple Model can be seen below in Figure 3.5 and Figure 3.6, respectively. The Corzine model has a total of 32 sensors and the simplified model has 20. However, in the future that number may reduce because of the minimal difference in the current readings of the sensors on the same line. This minimal difference may be due to the very small resistance of the power lines.

Figure 3.5 Sensor Placements in the Corzine Model

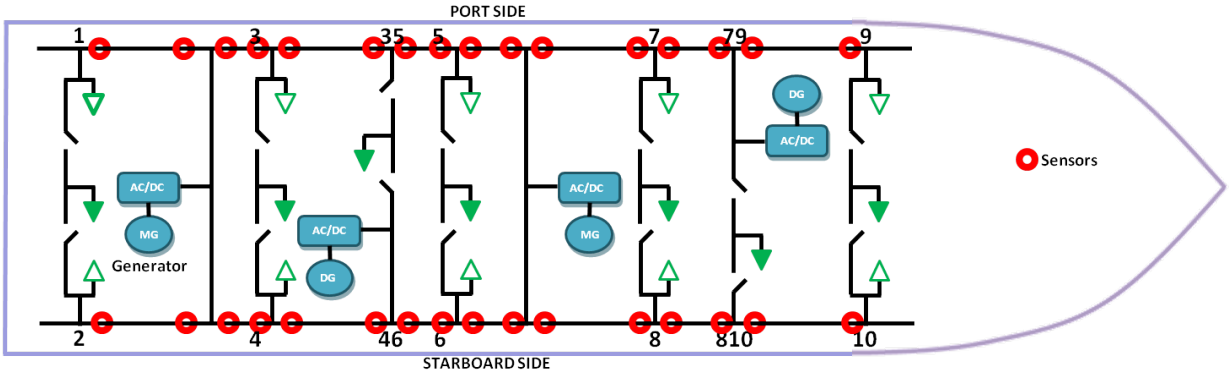

Figure 3.6 Sensor Placements in the Simple Model

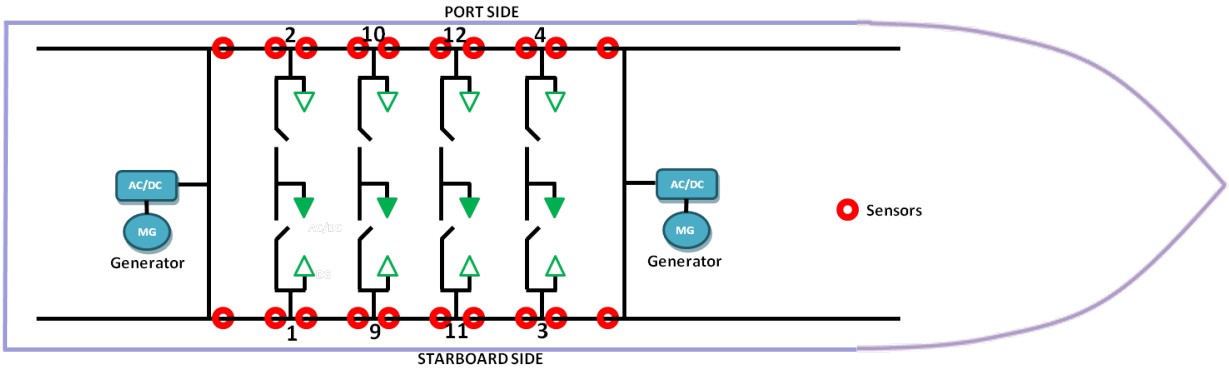

3.3.2 Current Data Collection

The current data collection is a very pivotal step in this study. There are many important aspects to consider when choosing how to collect the current data. The placement of the sensors and sampling rate of the sensors are among them. The sampling rate being too long could slow the algorithm down and the electric power system could be negatively affected. However, the sampling should not be too slow, because the location prediction could be incorrect; this is shown in Figure 3.7. The figure shows that if you sample faster than the current, data could be off. If you sample at a more correct rate, 80 ms, you could get more accurate data. In the figure the fault occurs at 40 ms and stays on the line until 50 ms.

Figure 3.7 Sensor Current in the Simple Model

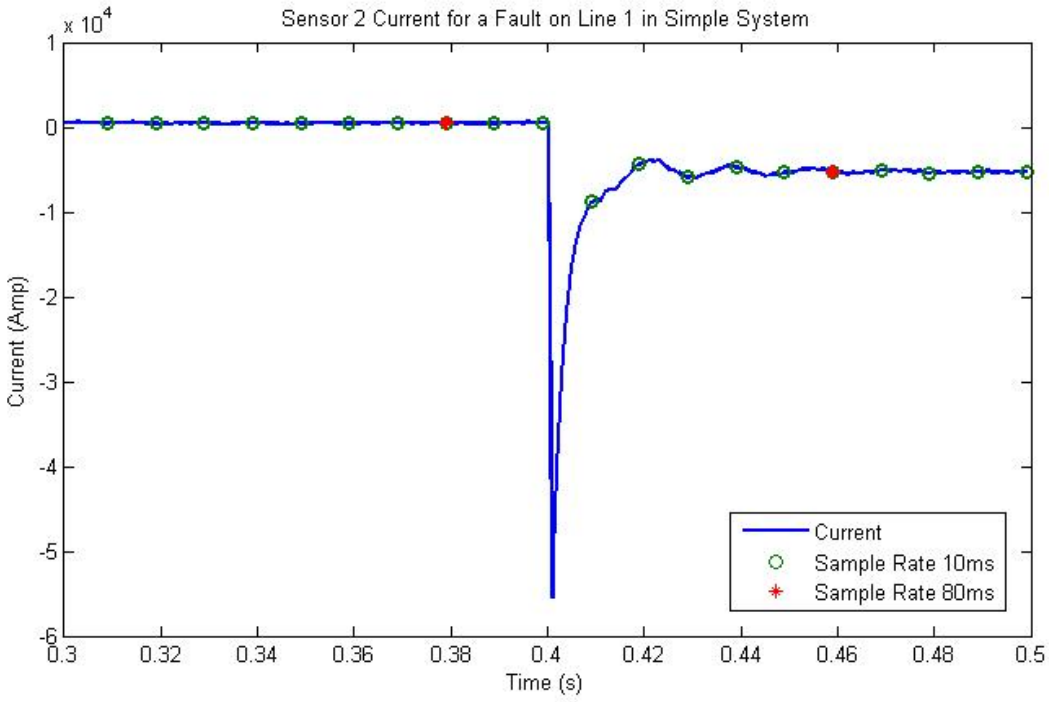

3.3.3 Analysis of Current Data

The sensor current data is collected for all single faults and all switching configurations. The simple model data histogram, below in Figures 3.8 and Figure 3.9, resembles mostly that of a Gaussian distribution. The difference between 100*R and 1000*R is that as the fault impedance grows the distribution of current moves toward the normal. This reason for this movement is the higher impedance causes less current in the system. This thought will be explored in Section 5.2.

The data for the Corzine ship shows that there are two main divisions in the data. One of these situations includes where the combination of a switching configuration and a fault do not affect the SPS enough that the fault currents at some sensors lie within the normal current regions. These regions are shown in an example, in Figure 3.10 and Figure 3.11, in red. As seen, the Histogram shows two regions and one region falls under the normal region. This is because of the high impedance and the switch configuration coincides so that the impact is minimal. The plots show that the high impedance faults that affect the system show a distribution that resembles a Gaussian distribution.

Figure 3.8 Sensor Current Histograms in the Simple Model (100R)

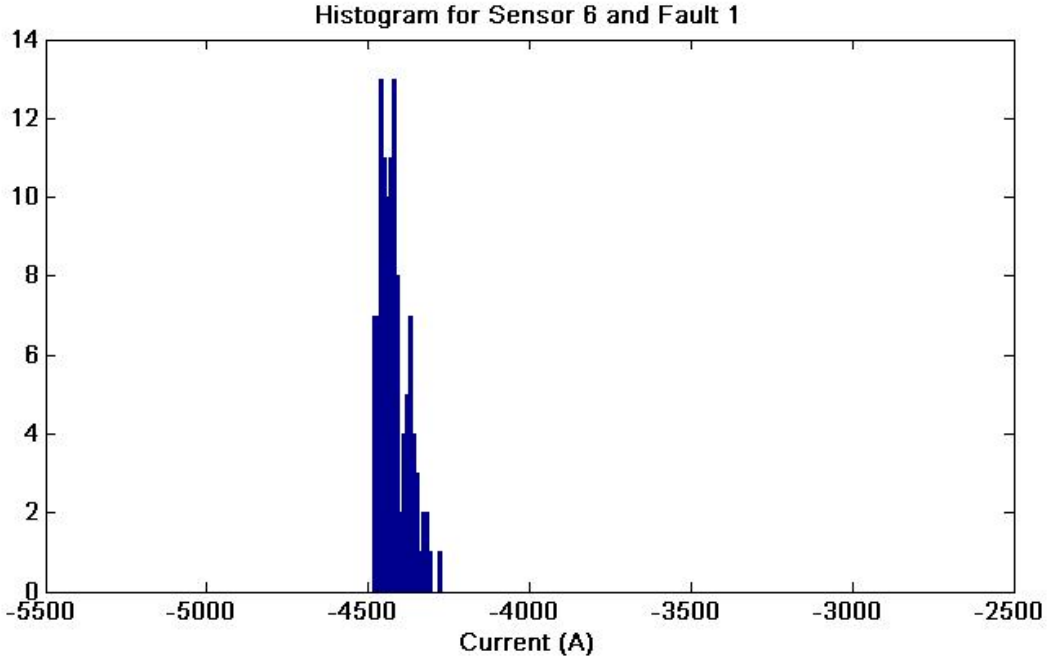

Figure 3.9 Sensor Current Histograms in the Simple Model (1000R)

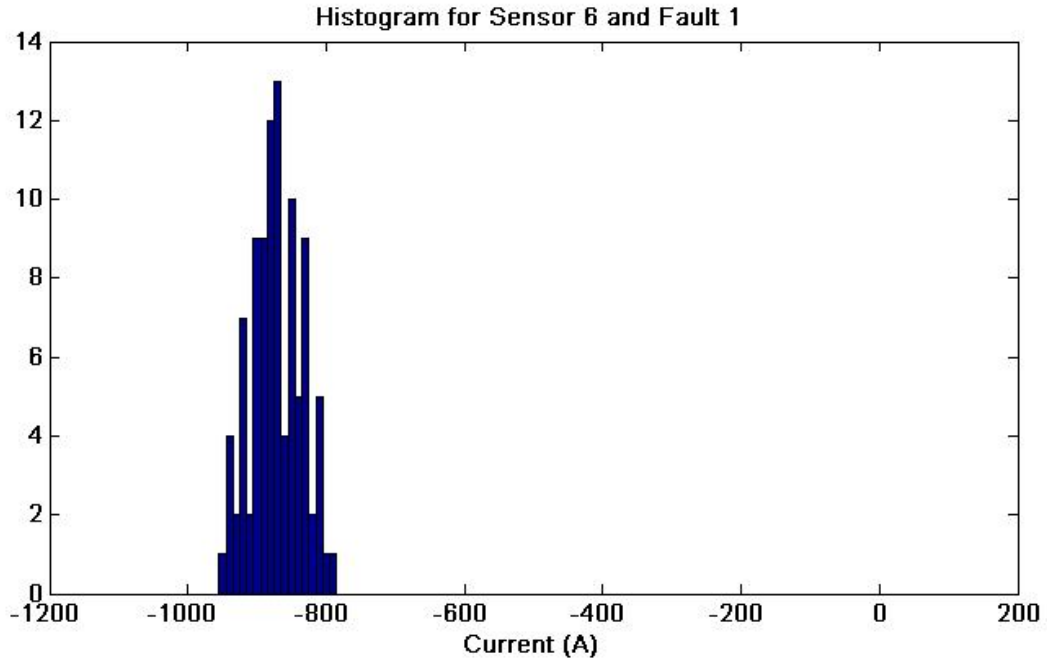

Figure 3.10 Sensor Current Histograms in the Corzine Model (100R)

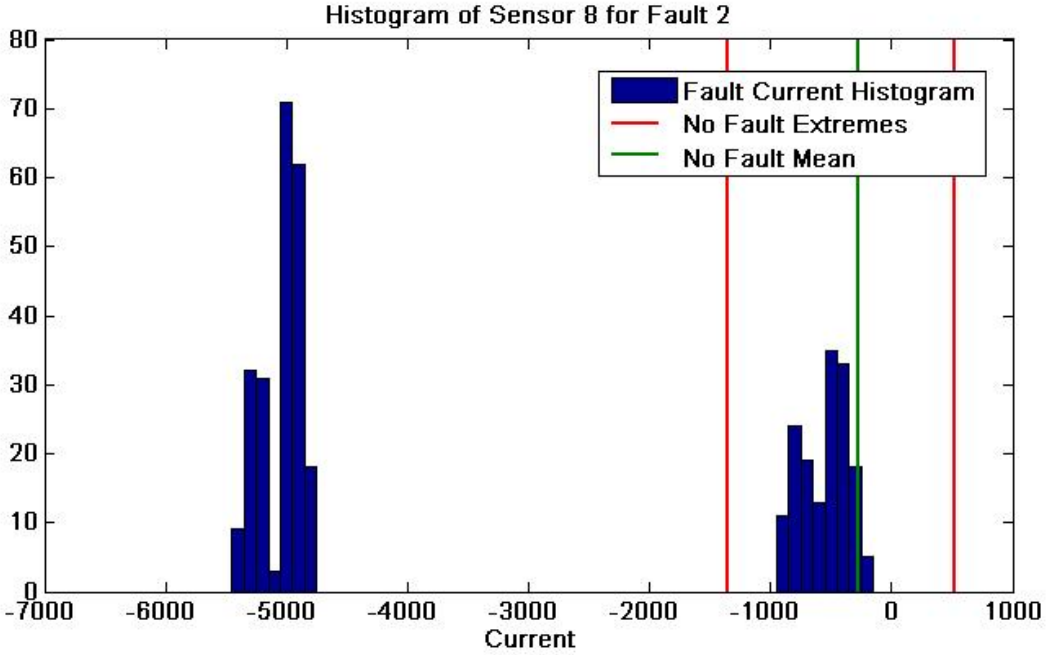

Figure 3.11 Sensor Current Histograms in the Corzine Model (1000R)

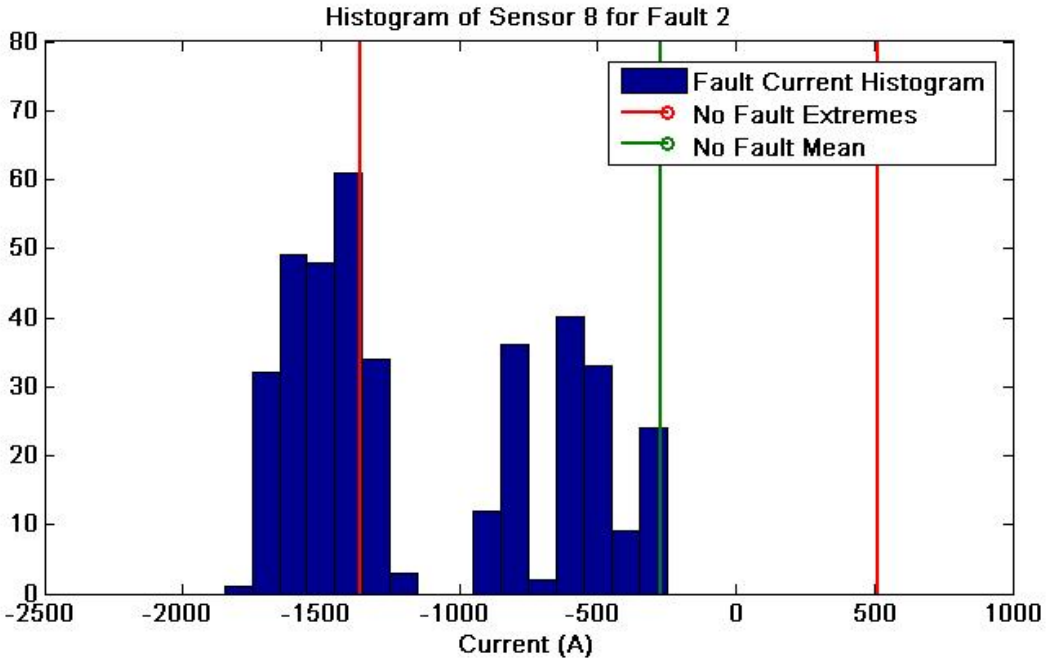

The distributions of the faults for sensor 8 and 100*R fault impedance, in the middle of the bus, can be seen in Figure 3.12 below. As you can see the currents for some faults, especially ones on the same line, have similar distributions to other faults. This is where sensor data fusion techniques can be applied to determine the likely fault location. However, the Corzine model presents a problem as bimodal distributions are formed. The second of the two distributions look similar to the normal distributions, as shown in Figure 3.13. These faults that occur in this range have limited effect on the system because the power equipment is meant to handle this type of current levels. Therefore, the faults that lie outside the normal distributions are used to determine the classification of the fault location.

Figure 3.12 Distributions of Sensor fault Currents in the Corzine Model (100R)

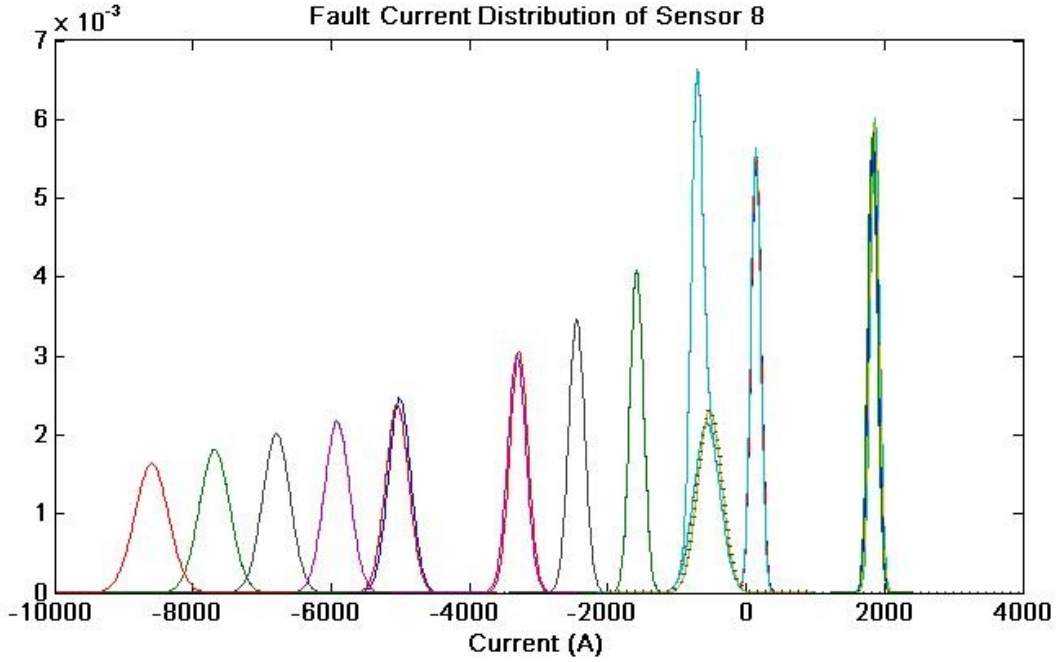

Figure 3.13 Comparison of Sensor Fault Current to the Normal Current Distributions

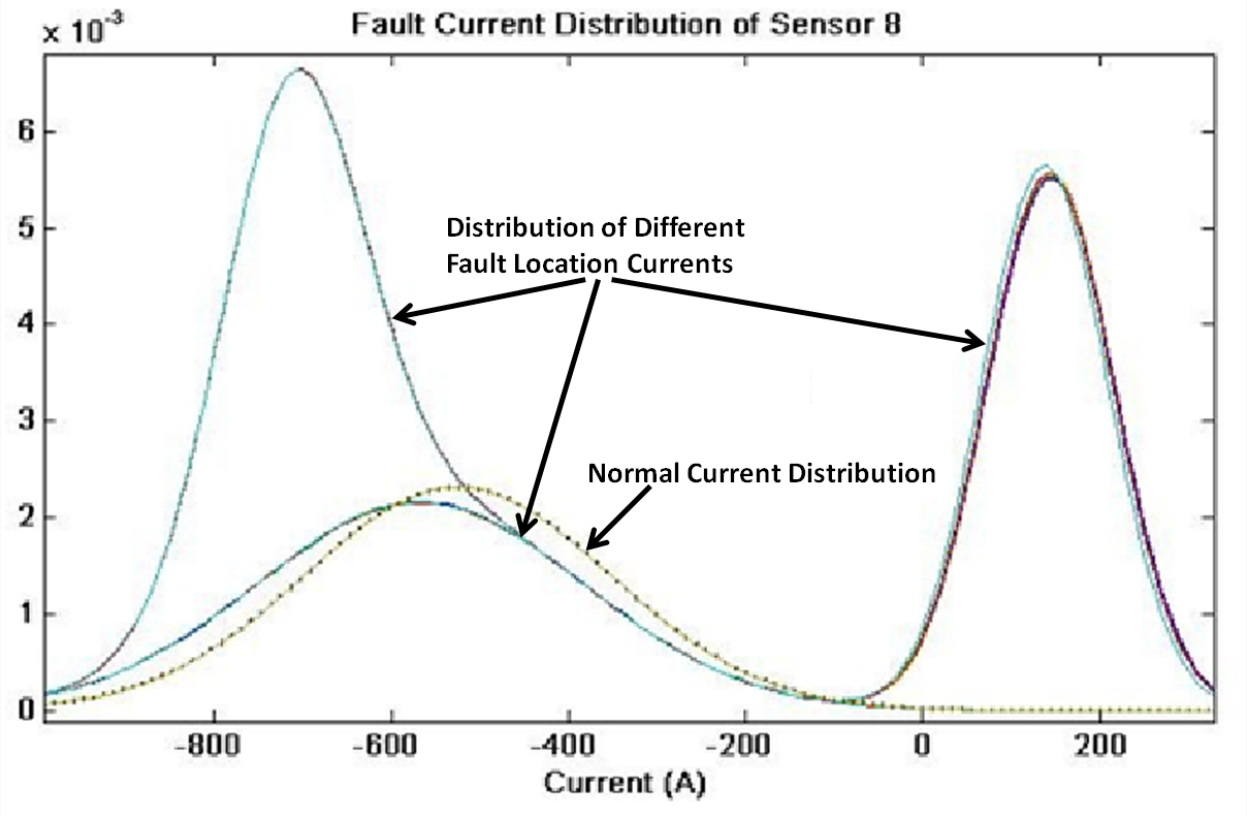

3.4 Summary

This chapter presented two models, the simple model and the Corzine model. The simple model is presented for development of methods and the Corzine is implemented to further test and develop those methods. Each model was simulated in MATLAB Simulink. The fault current data was collected and the distributions of the currents were analyzed. The next step is to develop the method to find the location of the faults in the system.

Chapter 4 - Bayesian Methods

Bayesian methods have been used to estimate specific types of faults in power equipment in [27][28]. The currents collected showed a distribution above that could be used to determine the most likely location for the fault. In this section, some Bayesian methods and simplification are discussed as explained in [29][30][31].

4.1 Maximum a Posteriori Estimation

Suppose that a sample of the sensor currents $i_1, i_2, \dots, i_N$ which are of the distributions shown above. The goal is to estimate the parameter or fault location $\boldsymbol{F}$. One of the most accurate ways to estimate the fault location parameter is the Maximum a Posteriori estimator. This estimator returns the parameter that maximizes the probability, $prob(\boldsymbol{F}|i_1, i_2, \dots i_N)$, as follows:

$$\boldsymbol{F}_{MAP} \leftarrow \underset{\boldsymbol{F}}{\operatorname{argmax}}\, prob(\boldsymbol{F}|i_1, i_2, \dots i_N) \quad (4.1)$$

The maximum a posteriori probability is described in Equation 4.2 below using Bayes theorem. This is basic estimator of the maximum a posteriori probability. On the right side of the equation, the numerator represents the likelihood of the currents given the fault location and the prior probability. The denominator is a normalization term, which ensures that the probability on the left integrates to unity. The denominator can be excluded when calculating the estimate.

$$prob(\boldsymbol{F}|I) = \frac{prob(I|\boldsymbol{F}) \times prob(\boldsymbol{F})}{prob(I)}, I = \{i_1, i_2, \dots i_N\}$$

The main problem with this calculation is the knowledge of prior probabilities of the fault location parameters. Since the prior probabilities are not known in this research, this estimation cannot be determined. Therefore, the maximum likelihood estimation is a better fit for this research.

4.2 Method of Maximum Likelihood

The first simplification considered in this research is the maximum likelihood estimation. The estimation is described in the equation below. The method estimates the fault based on the likelihood of each sensor current based on each fault location parameter. The fault location that maximizes this likelihood is chosen as the estimated fault location.

$$\boldsymbol{F}_{ML} \leftarrow \underset{\boldsymbol{F}}{\operatorname{argmax}}\, prob(i_1, i_2, \ldots i_N | \boldsymbol{F})$$

4.3 Simplifications of Maximum Likelihood

Further simplifications are made to make the computation faster and less complicated. The first assumption made is that the current distribution for each sensor for each fault is Gaussian. The distribution of these currents, seen in the figures in Chapter 3, resembles a normal Gaussian distribution. This assumption inserts Equation 4.4, below, into the maximum likelihood estimator.

$$prob(i_S | \boldsymbol{F}) \sim N(\mu_{\boldsymbol{F},S}, \Sigma)$$

The next simplification is the assumption that each sensor is conditionally independent. The joint density function can be written as the product of the individual probabilities, shown in the equation below:

$$\boldsymbol{F} \leftarrow \underset{\boldsymbol{F}}{\operatorname{argmax}} \prod_{S} prob(i_S|\boldsymbol{F})$$

The final simplification was fixing the standard deviation for each fault for each sensor. This simplification decreases the complication of each calculation. However, some accuracy is lost when this assumption is made.

$$prob(i_S|\boldsymbol{F}) \sim N(\mu_{\boldsymbol{F},S}, \sigma)$$

Chapter 5 - Proposed Approach to Fault Location Identification

After the explanation of the Bayesian methods, this section will describe the development, simplification, and modification of the proposed algorithm. All the algorithms described are developed in MATLAB. The main problems that need to be addressed are how to tell when there is a fault, complexity of the algorithm, and the adaptability of the algorithm.

5.1 Triggering the Fault Identification

The first problem when locating a fault is how to tell if a fault exists or doesn't exist. One way to tell if there is a fault is to check the change in currents. Since the sampling rate was chosen, it can be compared to the previous and present currents against a certain normal change in current for each sensor. The usual normal changes for each sensor in our situations would be only when the switches are opened or closed and the load configuration changes. The faults that are harmful to the power system, such as electronics, would cause abnormal rises in current. The rises in current would be greater than that of the normal changes.

So in this algorithm, the changes in current are constantly compared to the maximum current change due to normal conditions. The results using the trigger for each fault case are shown below in Table 5.1 as tested on both shipboard power models. The table shows the results of both models used in this research. It compares the precision of the method when determining the location at the ends of the power lines or just which power line has a fault. The Corzine model results are further split comparing the accuracy of faults that affect the system and all the faults which includes fault currents that fall under the normal range in current. As you can tell the trigger has little effect on the ML method using the covariance matrix. In fact, the affected parts are faults that are considered within normal range of current for all sensors. When using the

variances and a fixed variance is used, as explained later, the trigger has a minimal effect on the accuracy of the method, at the less than 2%. A detailed set of tables with the accuracy values for both the variances and fixed variances can be seen in Appendix A.

Table 5.1 Comparing Accuracy: Original Method and Addition of a Trigger

SPS Model	Resistance	Included Faults	Location	ML Accuracy (%)	Trigger and ML Accuracy (%)
Simple	100*R	All Faults	Lines	100.00	100.00
Simple	100*R	All Faults	Ends of Lines	85.66	85.66
Simple	1000*R	All Faults	Lines	100.00	100.00
Simple	1000*R	All Faults	Ends of Lines	84.77	84.77
Corzine	100*R	Outside of Normal Current	Lines	99.86	99.86
Corzine	100*R	Outside of Normal Current	Ends of Lines	84.15	84.15
Corzine	100*R	All Faults	Lines	61.74	59.17
Corzine	100*R	All Faults	Ends of Lines	51.13	49.80
Corzine	1000*R	Outside of Normal Current	Lines	100.00	100.00
Corzine	1000*R	Outside of Normal Current	Ends of Lines	86.40	86.40
Corzine	1000*R	All Faults	Lines	61.84	59.28
Corzine	1000*R	All Faults	Ends of Lines	52.44	51.22

5.2 Sweeping through All Possible Faults

The main problem of fault location impedances would be that when a fault happens, the impedance is not always immediately known. Therefore, an algorithm should accommodate any of the fault impedances that should occur. This research assumes two things about fault

impedances: lower impedances are quickly identified and taken care of before the algorithm takes place and higher impedances, above our range, have little effect on the system. Therefore, the range in which the algorithm needs to check is 100*R to 1000*R. The way that you sweep through, given the mean for each resistance will be different, is very important. The proposed method assumes that the mean and variances are linear and the move in toward the normal range as the resistance gets higher. The step size needed to seep through the impedances is tested in Table 5.2. The table shows that the algorithm is less accurate if fewer steps are taken. However, the difference between the two is less than 1%.

Table 5.2 Multiple Random Impedance Fault Accuracy

	Step Size	
Fault Impedance	*10R*	*100R*
123R	82.2	82
731R	82.0	79.6

5.3 Procedure and Results

Combining the two methods above, the proposed algorithm is seen below in Figure 5.1. The sensors are constantly updating the currents at a rate of 80ms. If the trigger is activated, then the algorithm steps through all possible faults and gets a possible fault location and probability that the fault is in that location. The trigger is explained below as if the change in current is greater than the normal change in current, ΔI_{NORMAL}. After this process, the fault location that has the highest probability is picked as the estimated fault location. The results of this method including the Trigger can be seen above in Table 5.1.

Figure 5.1 Full Process with Trigger and Fault Impedance Loop

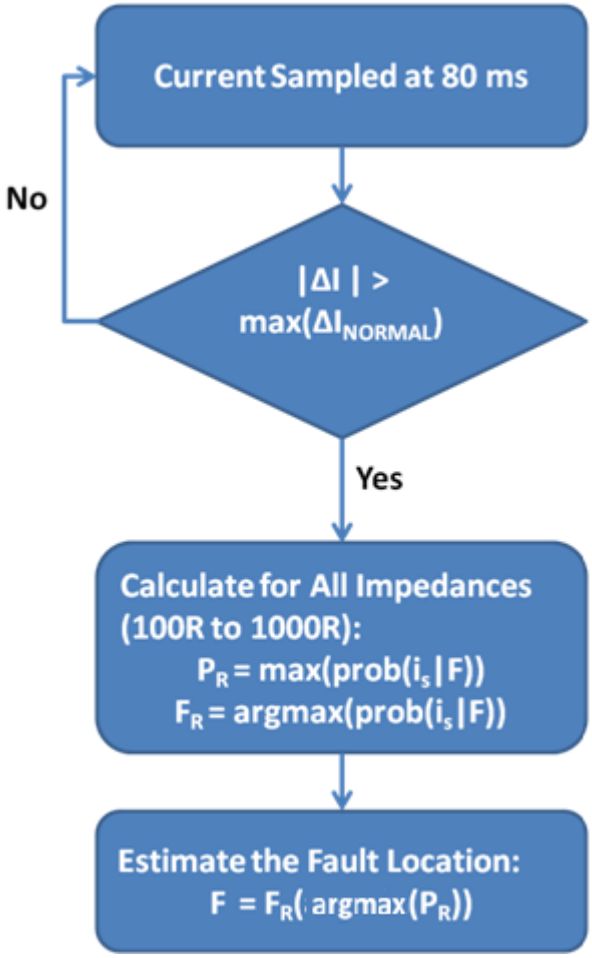

5.4 Simplification of the Algorithm

In fault location identification, the idea is to find, isolate and repair the fault as fast as possible. So, the least amount of time that the location process takes is better for the power system. The best way to speed up the process is to reduce the calculation time. This includes decreasing the storage needed to calculate the location and the total amount of calculations need to make the estimate.

5.4.1 Fixed Variance

An excellent way to reduce the amount of calculations and storage is to reduce the number of parameters that need to be calculated. Since the variances needed to be calculated for every step or every impedance in the proposed method, it would be an advantage to eliminate this calculation. This fixed variance reduces the calculation to determining the minimum squared distance to the next fault for each sensor. The results are compared with using variances for each fault on each sensor in Table 5.3.

As can be seen in the table, this reduction has little effect on the simple model. The only difference is the end of power lines estimate. The Corzine model shows that there is little effect when changing to just fixed variance.

Table 5.3 Comparing Accuracy: Multiple Variances and Fixed Variance

SPS Model	Resistance	Included Faults	Location	Variances Accuracy (%)	Fixed Variance Accuracy(%)
Simple	100*R	All Faults	Lines	100.00	100.00
Simple	100*R	All Faults	Ends of Lines	79.85	76.54
Simple	1000*R	All Faults	Lines	100.00	100.00
Simple	1000*R	All Faults	Ends of Lines	76.90	75.52
Corzine	100*R	Outside of Normal Current	Lines	100.00	100.00
Corzine	100*R	Outside of Normal Current	Ends of Lines	78.11	78.11
Corzine	100*R	All Faults	Lines	61.88	61.82
Corzine	100*R	All Faults	Ends of Lines	47.57	48.38
Corzine	1000*R	Outside of Normal Current	Lines	100.00	100.00
Corzine	1000*R	Outside of Normal Current	Ends of Lines	74.20	46.75
Corzine	1000*R	All Faults	Lines	61.91	61.96
Corzine	1000*R	All Faults	Ends of Lines	45.29	45.63

5.4.2 Active Sensors

In order to reduce the number of calculations that it takes to make the fault location estimation, a logical step is to only use important sensors in the calculations. The sensors that are affected with current greater than that of the normal change in current can be used. This would reduce the number of calculations because not all the sensors are needed for their information in order to make the decision. Table 5.4 below shows the correct location estimation percentage of the method when using all the sensor data compared to that of the method using only the activated sensors.

Table 5.4 Comparing Accuracy: All Sensors and Active Sensors

SPS Model	Test Set Resistance	Included Faults	Location	All Sensors Accuracy (%)	Active Sensors Accuracy (%)
Simple	100*R	All Faults	Lines	100.00	100.00
Simple	100*R	All Faults	Ends of Lines	85.66	75.90
Simple	1000*R	All Faults	Lines	100.00	100.00
Simple	1000*R	All Faults	Ends of Lines	84.77	49.49
Corzine	100*R	Outside of Normal Current	Lines	99.86	93.79
Corzine	100*R	Outside of Normal Current	Ends of Lines	84.15	72.93
Corzine	100*R	All Faults	Lines	61.74	55.54
Corzine	100*R	All Faults	Ends of Lines	51.13	43.16
Corzine	1000*R	Outside of Normal Current	Lines	100.00	73.27
Corzine	1000*R	Outside of Normal Current	Ends of Lines	86.40	47.89
Corzine	1000*R	All Faults	Lines	61.84	43.41
Corzine	1000*R	All Faults	Ends of Lines	52.44	28.30

5.5 Summary

In this chapter, a method for fault location identification is presented. A trigger is devised to start the method when a fault occurs. Then, the method is further simplified to decrease the speed in which it takes to locate the fault. The fist simplification developed was to fix the variances. This simplification decreased the accuracy a little but not much. The second simplification was using only active sensors information to determine the location of the fault. Overall the method developed was accurate in determining the location of the fault. The next chapter tests the method that was developed.

Chapter 6 - Performance and Testing of the Developed Algorithm

The next step in the process is to test this method. When a fault happens in the system, the sensors have no knowledge of the impedance of the fault. Therefore, the best way to test the method is to simulate random faults. Another way to test the system is with multiple faults. The final way to test would be a change in load. If the load changes in a system, the currents could change without the knowledge of the sensor. All three of these tests need to be evaluated for completeness of this method.

6.1 Random Fault Impedances and Multiple Faults

The first two tests of the algorithm are random fault impedances in multiple locations. The two fault impedances that were chosen at random were 123*R and 731*R. In this test, those two impedances are simulated at random locations and could be simulated up to two locations at the same time. These multiple fault locations should test the location algorithm to the brim in Table 6.1, the results of the test of random faults at multiple locations in the Corzine model is shown. The step size referred to in the table is the step size when looping from 100*R to 1000*R, explained above in Section 5.2. As can be seen in the table the algorithm is a little more accurate for the 123*R than the 731*R. However, the difference is small and the method does a pretty good job of identifying the fault location along the power system.

Table 6.1 Multiple Random Impedance Fault Accuracy

	Step Size	
Fault Impedance	*10R*	*100R*
123R	82.2	82
731R	82.0	79.6

6.2 Simulating Imperfect Sensors

Most practical sensor readings have a relative error in practice. Therefore, to test this theoretically, noise need to be added to the sensors. For the worst-case scenario, uniform distribution random noise is added to the sensor within ±5% of the simulated value of the sensors. As shown below in Table 6.2, the fully developed method, using active sensors and a fixed variance the noise, does not affect the accuracy by much. In fact, in some cases the accuracy is increased by a little. This is due to the limited test sample, and if more samples were run, the data should reflect a small decrease in accuracy with added noise. However, the overall effect on the method is small.

Table 6.2 Comparing Accuracy: Fixed Variance Active Sensors With and Without Noise

Test Set Resistance	Included Faults	Location	Without Noise (%)	Added Noise (%)
100*R	Outside of Normal Current	Lines	91.23	92.31
100*R	Outside of Normal Current	Ends of Lines	72.61	67.31
100*R	All Faults	Lines	54.01	56.18
100*R	All Faults	Ends of Lines	42.95	41.07
1000*R	Outside of Normal Current	Lines	72.30	72.09
1000*R	Outside of Normal Current	Ends of Lines	46.75	46.66
1000*R	All Faults	Lines	42.80	42.72
1000*R	All Faults	Ends of Lines	27.66	27.58

6.3 Unbalanced Loads along the SPS

The one thing that has not been discussed in this research thesis so far is what if the load shifts. Shifts in the load can happen during normal operations. A load at one position on the grid may switch to another position over a period of time. Two different types of load distributions are tested. On one of the distributions a higher percentage of the load is toward the center of the ship, i.e., a center biased load. Another distribution that is tested is a right biased load, with a higher percentage of the load distributed to the right of the ship. The center and right distributed loads are represented in Figures 6.1 and 6.2. Each figure shows the percentage of the total load that is included in the areas encircled. Also noted is that the vital, semi-vital, and non-vital loads keep their ratios of the load within the encircled areas. That is, since the semi-vital consumes twice the power as the other two loads originally, the same applies during these simulations and tests.

Figure 6.1 Central Biased Load Distribution

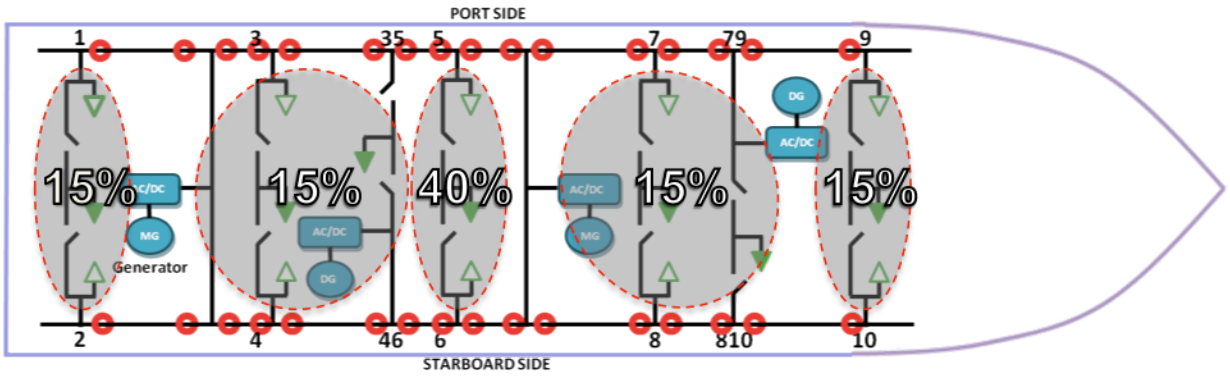

Figure 6.2 Right Biased Load Distribution

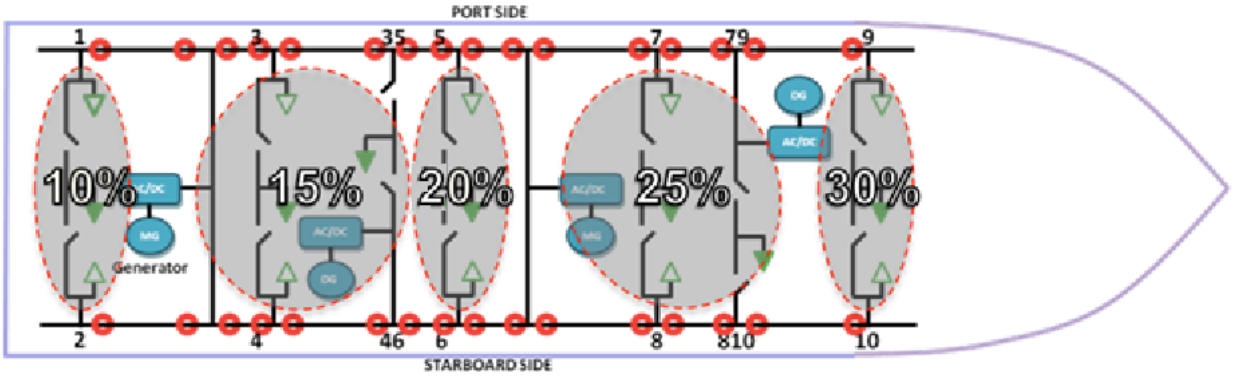

These distributed loads are tested with the same method as described above, with the same means and with the same deviations. This process is used as well to test the step size when looping through the possible impedance faults. The results of these tests are shown below in Table 6.3. As you can tell, the faults in the load distribution that favors the center of the SPS are located with a little less accuracy but still located at a respectable rate. However, the method is not as accurate with the right biased load distribution. The accuracy decreases because the current means move with the load distribution and the method does not account for this change in current values.

Table 6.3 Unbalanced Load Fault Accuracy

	Step Size	
Load Bias	*10R*	*100R*
Center (100R)	84.0	83.8
Right (100R)	14.0	13.6

6.4 Online Training for Better Results

The method needs a way to adapt to the change in loads in the SPS. If the loads are changing, the parameters in the location, such as the means, should be changing along with the load shifts. In this part of the research, a decreased load distribution is used to test if the method can adjust to a shift in load. In Figure 6.3, the percentages shown are the amount of the original load distribution. For example, the far left load zone is decreased to 50% of its original load value.

Figure 6.3 Right Biased Decreased Load

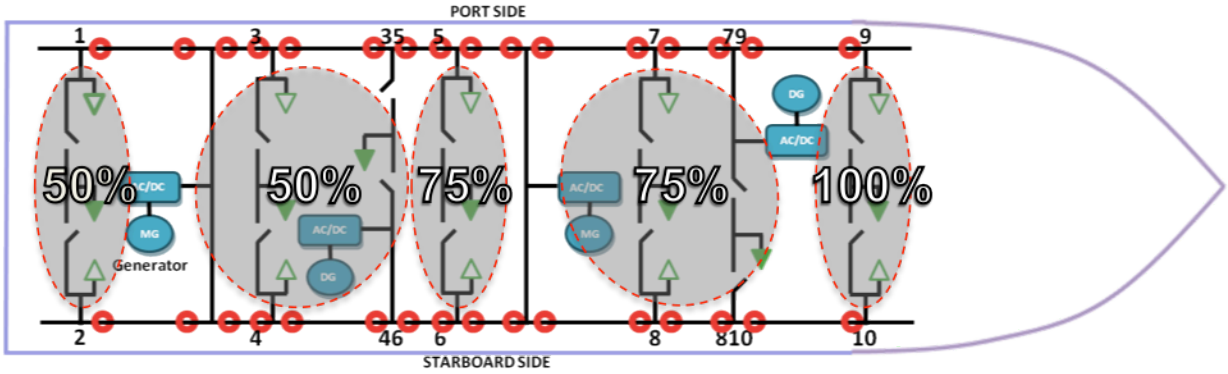

The situation being tested here is that a standard load distribution is running and the means of the fault situations for each sensor is already known. After that, the load distribution change and some of the loads, toward the left side of the model, are decreased. The model needs to be able to adapt to this situation in order to have higher accuracy. In this situation, the same algorithm is used with some modifications.

Since the fault impedance is not known in any fault situation case, the fault impedance needs to be estimated. In this method of online training, the previously computed probabilities of fault impedances are used. The method steps from 100*R impedance to 1000*R computing the

most likely fault impedance for each. The online method uses these probabilities to estimate the fault impedance. The following equations show the method used to slowly update the means of the Gaussians.

$$\rho_{R_1} = \frac{R_{Fault} - R_1}{R_2 - R_1} \quad and \quad \rho_{R_2} = \frac{R_2 - R_{Fault}}{R_2 - R_1} \tag{6.1}$$

$$\Delta\mu_{R_1} = \epsilon\rho_{R_1}(I_{Fault} - \mu_{R_1}) \tag{6.2}$$

$$\Delta\mu_{R_2} = \epsilon\rho_{R_2}(I_{Fault} - \mu_{R_2}) \tag{6.3}$$

$$\mu_{R_1} \leftarrow \mu_{R_1} + \Delta\mu_{R_1} \quad and \quad \mu_{R_2} \leftarrow \mu_{R_2} + \Delta\mu_{R_2} \tag{6.4}$$

In the equations above, the resistance R_1 is equal to 100*R and the resistance R_2 is equal to 1000*R. Equation 6.1 describes a fraction ρ for each resistance on how much they should update the means. Equation 6.2 calculates the difference between the current of the fault and the mean of each mean. Next, this amount is portioned to each resistance using the fraction described in Equation 6.1. Then, ϵ is used to make sure that the online method does not overreact to outliers. In this research ϵ is set to 0.01. However, testing was needed to find an optimum value for this parameter.

The results for this online method are shown below in Table 6.4. The means from the original balanced load are used as the means in the beginning and the online method is run. 500 random impedances at randomly selected locations are simulated with different switching configurations. The means are trained with two thirds of the faults simulated. In the end, the

means calculated are tested with the last third of the faults and the 100*R and 1000*R faults simulated beforehand. The results are shown in Table 6.4. The online method improves the results by a significant amount and with more simulations the estimation's accuracy could become greater.

Table 6.4 Comparing Accuracy: Before and After Online Training for Load Shifted System

Test Set Resistance	Full Implement ML (%)	Online Training (%)
100*R	14.0	84.4
1000*R	12.2	63.7
Random	n/a	78.8

6.4 Fault Impedances Outside the Specified Range

The final situation that needs to be tested is what if the fault impedance happens to be outside of the range set. The set range of 100*R to 1000*R was found during testing to be about the right range. However, the question still remains as to what the method will decide if the impedance of a fault falls outside that range and the preexisting assumption that small impedances are found quickly and isolated does not work. For this situation, 50*R is used to test the method. The other situation is that a higher impedance fault occurs. For this situation, 1250*R is chosen to show the estimate of the method. Table 6.5 shows the results.

Table 6.5 Outside Impedance Range Fault Accuracy

Test Set Resistance	Included Faults	Location	Accuracy (%)
50*R	Outside of Normal Current	Lines	90.4139
50*R	Outside of Normal Current	Ends of Lines	64.147
50*R	All Faults	Lines	53.4668
50*R	All Faults	Ends of Lines	37.9639
1250*R	Outside of Normal Current	Lines	18.9611
1250*R	Outside of Normal Current	Ends of Lines	9.8395
1250*R	All Faults	Lines	11.2061
1250*R	All Faults	Ends of Lines	5.8105

6.5 Summary

Multiple tests were developed to determine the robustness of the method. The first method was to simulate multiple random impedance faults. The method located the faults with good accuracy. The second test was to simulate imperfect sensors. The method was not affected by this addition of noise to the sensors. The third test was shifts in the load. Two load distributions were developed and tested, right and central biased. The method was accurate for the central biased load. However, the right biased load provided problems for the method. An online method was developed to adapt to changes in load to help this problem. This online method was then tested with random impedances. The method produced an increase in accuracy for shifts in load. The final test was impedances outside the range specified. The method accurately found faults under the impedance range. However, the impedances above the impedance range were a problem. In Chapter 7, the method is compared to other presented methods.

Chapter 7 - Comparing with other Methods

There are many other methods to compare these results out there. One way to test some of these methods is to use WEKA. WEKA is a data mining toolbox that uses Java and data files to allow you to use many of the methods out there [32]. In this comparison, multilayered perceptron (MLP) network and a simple Classification And Regression Tree (SimCART) are simulated.

Multilayered perceptron network is a neural networks model that intakes data and maps to an output set. MLPs use back propagation to train the network. Back propagation is a form of supervised learning where the output of the network is compared to the expected result and adapting the network based on this error.

A simple Classification And Regression Tree (CART) is a decision tree that compares the inputs to set values and returns a decision as the output. Each node of the tree compares one of the inputs to a set value and then, based on this comparison, a decision is made to move on to the next node. The ends of the tree are the decided classification. In Figure 7.1, a simple CART tree is shown.

Figure 7.1 Simple CART Tree Example

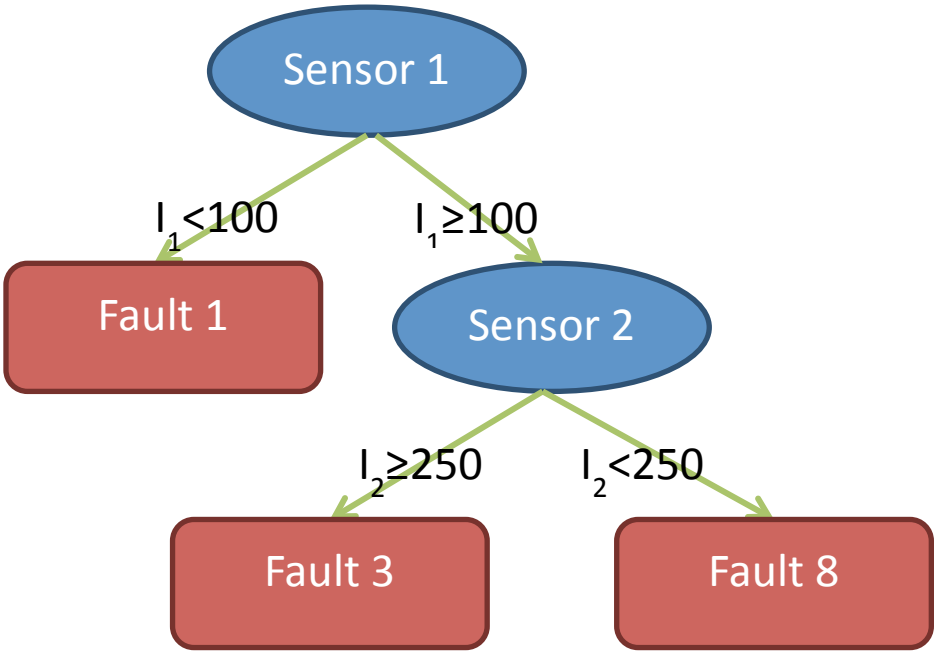

Table 6.6 shows the accuracy of those methods compared to the proposed method. The first two tests are the methods trained with 100*R and 1000*R and then tested with each set of 100*R and 100*R. The results show that the tree was the worst and the proposed method outperformed the MLP. The last set is the random faults. The online method and the two WEKA methods trained with 66% of the 500 random faults created earlier and then trained with 33% of that test set. The results show that the developed method determined the location of the fault better than the other methods.

Table 7.1 Comparing Method to MLP and SimCART

Test Set Resistance	Full Implement ML (%)	MLP (%)	SimCART Tree (%)
100*R	91.23	80.9	75.9
1000*R	72.30	70.6	62.1
Random	78.80	76.0	72.0

Chapter 8 - Discussion and Conclusion

An approach was designed to determine the location of a high impedance ground fault in a DC shipboard power system. Two different shipboard power system models were used to determine the effectiveness of the method. One of the models used to formulate a model and a more complex model to test the rigidness of the model. Each of these power systems contains generators, AC to controlled DC converters, power lines, and loads. The power systems are simulated in MATLAB Simulink using SimPowerSys toolbox.

Sensors placed on power lines recorded the line currents. The currents are collected for different load variations. These currents were then used to determine the location of a fault. Multiple Bayesian methods are used to determine the estimated location of a fault. Maximum likelihood is used to with Gaussian distributions of the currents in order to determine this location. The calculation of the maximum likelihood estimate is then simplified using fixed variances and only activated sensors. Activated sensors are sensors that recognize that the fault has occurred or their recorded current is greater than the current during normal situations. This method showed positive results for the originally proposed load system, evenly distributed throughout the ship.

Further tests were needed to test the method. The first test was random fault impedances. This test was introduced because when a fault occurs in the system the impedance is normally not known. For this situation, an algorithm is designed to loop through the possible high impedance faults and determine the most likely location of the fault. The next situation to test was a shift in load. An online method was introduced to adapt to shifting loads. This method helped the accuracy of the algorithm in shifting loads. When comparing the results to other

methods, multi-layered perceptron networks and classification trees, the final online training program produces higher accuracy after training.

There are many things that need to be further considered in the future research. This includes exploring if a sensor is lost in the same event of a fault how would the algorithm react. Other possible implementations include using the voting and Dempster-Schafer theories to determine the locations of the faults. These methods could be more accurate in their assessment of the sensor data in order to determine the fault location. Also, local decisions could be made to determine the fault location faster and act locally to protect loads and equipment near the sensors. Some of the future directions are outlined in Chapter 9.

Chapter 9 - Future Research

There are many possible expansions to this work. The Gaussians that are found in this work could help a sensor make decisions locally and protect the loads around the sensor. Voting systems and Dempster-Shafer belief algorithm could be implemented as well. The system also sets up well for the implementation and testing of the many voting systems available. Another possible exploration could be the decentralization of the method.

9.1 Voting

A voting system is a natural fit for this research. The sensors could represent voters and the fault locations would be the candidates. Many voting systems exist that could be modified, implemented and tested in this system. Various methods should be tested in order to choose the best voting system for this purpose. Each of these methods could possibly be implemented using fuzzy logic. These methods could be applied in a distributed decision making scheme to determine the fault location.

9.2 Dempster-Shafer Theory

Another method that could be compared to the proposed method is the Dempster-Shafer Theory. The theory combines evidence from different sources to create a degree of belief of certain events. Each sensor could send degrees of beliefs in fault locations and a sensor fusion method could combine that information in order to decide a centralized belief in a fault location. Like voting theory discussed above, this method could be modified for distributed decision making to decide the fault location. Examples of this method being modified for other applications are included in [33].

9.3 Decentralized Methods

Complex systems, such as a shipboard power system, can cause some more problems that would be better served locally to the problem rather than centrally located. The method that is produced in this research is centrally decided, meaning that the sensors send their information to a central location, a central processing unit, and the fault is then located, as seen in Figure 8.1. However, the fault location and isolation process could be sped up with a more distributed decision-making, as seen in Figure 8.2 and explained in [34]. A sensor could decide the location of a fault based on the accessible information, its current data and maybe some neighbors. Then, the sensor could isolate the fault faster with locally controlled equipment. Rules could be made as to when a sensor could make these decisions and a possible centralized decision could come later. However, a local decision could improve the time in which it takes to respond to a possible fault.

Figure 8.1 Centralized Decision Making Architecture

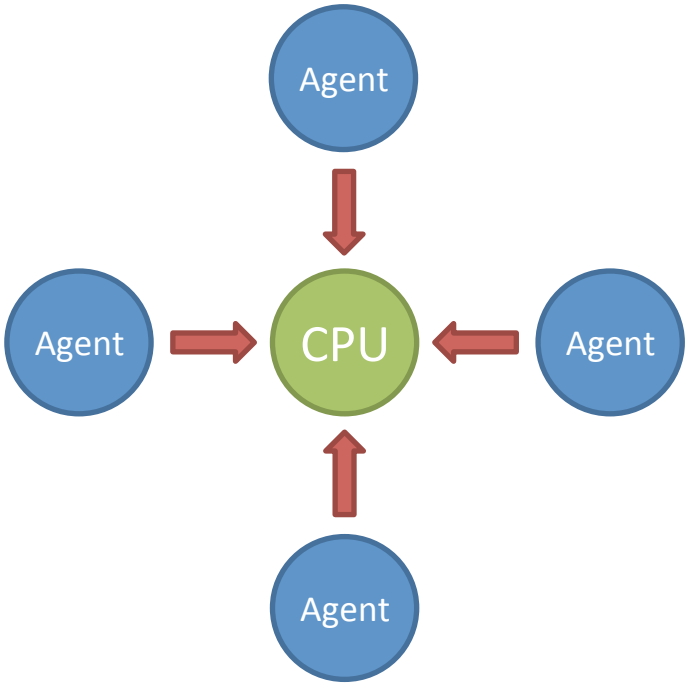

Figure 8.2 Decentralized Decision Making Architecture

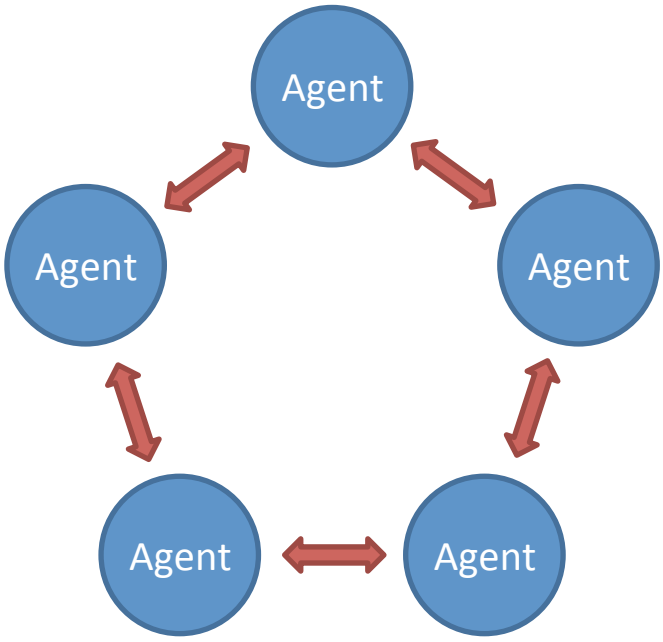

References

[1] M.C. Ahn, H. Kang, D.K. Park, Y.S. Yoom, S.J. Lee, T.K. Ko, "The Short-Circuit Characteristics of a DC Reactor Type Superconducting Fault Current Limiter With Fault Detection and Signal Control of the Power Converter", *IEEE Trans. on Applied Superconductivity*, vol. 15, no. 2, pp. 2102-2105, June 2005.

[2] S.H. Kang, Y.J. Ahn, Y.C. Kang, S.R. Nam, "A Fault Location Algorithm Based on Circuit Analysis for Untransposed Parallel Transmission Lines", *IEEE Tans. on Power Delivery*, vol. 24, no. 4, pp. 1850-1856. Oct 2009.

[3] Z.Y. He, R.K. Mai, W. He, Q.Q. Qian, "Phasor-measurement-unit-based transmission line fault location estimator under dynamic conditions", *IET Generation*, Transmission, and Distribution, vol. 5, no. 11, pp. 1183-1191, Nov 2011.

[4] Z. He, L. Fu, S. Lin, Z. Bo, "Fault Detection and Classification in EHV Transmission Line Based on Wavelet Singular Entropy", *IEEE Tans. On Power Delivery*, vol. 25, no. 4, pp. 2156-2163, Oct 2010.

[5] Z. He, J. Zhang, W. Li, X. Lin, "Improved Fault-Location System for Railway Distribution System Using Superimposed Signal", *IEEE Trans. On Power Delivery*, vol. 25, no. 3, pp. 1899-1911, July 2010.

[6] R. Jayabalan, B. Fahimi, "Fault diagnostics in naval shipboard power system for contingency management and survivability", *Electric Ship Technology Symposium*, pp, 108-111, 2005.

[7] O.M.K.K. Nanayakkara, A.D. Rajapakse, R. Wachal, "Location of DC Line Faults in Conventional HVDC Systems With Segments of Cables and Overhead Lines Using Terminal Measurements", *IEEE Trans. on Power Delivery,* vol. 27, no. 1, pp. 279-288, Jan 2012.

[8] L. Tang, B.T. Ooi, "Locating and Isolating DC Faults in Multi-Terminal DC Systems", *IEEE Tans. on Power Delivery,* vol. 22, no. 3, pp. 1877-1884, July 2007.

[9] Y. Pan, P.M. Silveira, M. Steurer, T.L. Baldwin, P.F. Ribeiro, "A Fault Location Approach for High-Impedance Grounded DC Shipboard Power Distribution Systems", *IEEE Power and Energy Society General Meeting,* pp. 1-6, July 2008.

[10] B.M. Aucoin, R.H. Jones, "High impedance Fault Detection Implementation Issues", *IEEE Trans. on Power Delivery*, vol. 11, no. 1, pp. 139-148, Jan 1996.

[11] M. Michalik, W. Rebizant, M. Lukowicz, L. Seung-Jae, K. Sang-Hee, "High-Impedance Fault Detection in Distribution Networks with Use of Wavelet-Based Algorithm", *IEEE Trans. on Power Delivery*, vol. 21, no. 4, pp. 1793-1802, Oct 2006.

[12] M. Sarlak, S.M. Shahrtash, "High Impedance Fault Detection using Combination of Multi-Layer Perceptron Neural Networks Base on Multi-Resolution Morphological Gradient Features of Current Waveform", *IET Generation, Transmission & Distribution*, vol. 5, no. 5, pp. 588-595, May 2011.

[13] Y. Pan, M. Steurer, T.L. Baldwin, "Ground Fault Location Testing of a Noise-Pattern-Based Approach on an Ungrounded DC System", *IEEE Trans. on Industry Applications*, vol. 47, no. 2, pp. 996-1002, Mar 2011.

[14] G.L. Kusic, "State Estimation and Fast Fault Detection For Ship Electrical Systems", *Electric Ship Technologies Symposium*, 2007, pp. 209-214.

[15] E. Christopher, M. Sumner, D. Thomas, F. de Wildt, "Fault Location for a DC Zonal Electrical Distribution Systems using Active Impedance Estimation", *Electric Ship Technologies Symposium (ESTS)*, 2011, pp. 310-314.

[16] C. Kim, "Detection and location of intermittent faults by monitoring carrier signal channel behavior of electrical interconnection system", *Electric Ship Technologies Symposium*, pp. 449-455, 2009.

[17] N.K. Chanda, Y. Fu, "ANN-based fault classification and location in MVDC shipboard power systems", *North American Power Symposium*, pp. 1-7, 2011.

[18] A.J. Mair, E.M. Davidson, S.D.J. Mcarthur, "Machine learning techniques for diagnosing and locating faults through the automated monitoring of power electronic components in shipboard power systems", Electric Ship Technologies Symposium, pp. 469-476, 2009.

[19] Padamati, K.R, N.N. Schulz, A.K. Srivastava, "Application of Genetic Algorithm for Reconfiguration of Shipboard Power System", *North American Power Symposium*, pp. 159-163, 2007.

[20] Y. Pan, P.M. Silveira, M. Steurer, T.L. Baldwin, P.F. Ribeiro, "A Fault Location Approach for High-Impedance Grounded DC Shipboardm Power Distribution Systems", *IEEE Power and Energy Society General Meeting,* pp. 1-6, July 2008.

[21] Y. Pan, M. Steurer, T. Baldwin, "Feasibility study of noise pattern analysis based ground fault locating method for ungrounded DC shipboard power distribution systems", *Electric Ship Technologies Symposium*, pp. 18-22, 2009.

[22] H. Limin, Z. Yongli, L. Ran, Z. Liguo, "Novel method for power system fault diagnosis based on Bayesian networks", *International Conference on Power System Technology*, vol. 1, pp. 818-822, 2004.

[23] N. Qianwen, W. Youyuan, "An Augmented Naive Bayesian Power Network Fault Diagnosis Method Based on Data Mining", *Power and Energy Conference*, pp. 1-4, 2011.

[24] C.F. Chien, S.L. Chen, Y.S. Lin, "Using Bayesian network for fault location on distribution feeder", *IEEE Trans. on Power Delivery*, vol. 17, no. 3, pp. 785-793, July 2002.

[25] J. Billo, "Models and Methods for Shipboard Power System Reconfiguration", *Thesis for University of Texas*, 2003.

[26] K. Corzine, *Electric Ship Research and Development Consortium*, Missouri University of Science and Technology, 2010.

[27] W. Yongqiang, L. Fangcheng, L. Heming, "The Fault Diagnosis Method for Electrical Equipment Based on Bayesian Network", *Proceedings of the Eighth International Conference on Electrical Machines and Systems*, vol. 3, pp. 2259-2261, 2005.

[28] N. Qianwen, W. Youyuan, "An Augmented Naive Bayesian Power Network Fault Diagnosis Method Based on Data Mining", Asia-Pacific Power and Engineering Conference, 2011, pp. 1-4.

[29] H. Akaike, "Information theory and an extension of the maximum likelihood principle", *Second International Symposium on Information Theory*, pp. 267-281, 1973.

[30] M. DeGroot, "Optimal Statistical Decisions", *McGraw-Hill*, 1970.

[31] G. L. Gauvain, C. H. Lee, "Maximum a posteriori estimation for multivariate Gaussian mixture observations of Markov chains", *IEEE Trans. on Speech and Audio Processing*, vol. 2, no. 2, pp.291-298, Apr 1994.

[32] M. Hall, E. Frank, G. Holmes, B. Pfahringer, P. Reutemann, I.H. Witten, "The WEKA Data Mining Software: An Update", *SIGKDD Explorations*, vol. 11, no. 1, 2009.

[33] H. Jeung, W. Jiangfeng, "Bayesian and Dempster-Shafer target identification for radar surveillance", *IEEE Trans. on Aerospace and Electric Systems*, vol. 36, no. 2, pp. 432-447, Apr 2000.

[34] S. Roy, K. Herlugson, A. Saberi, "A control-theoretic approach to distributed discrete-valued decision-making in networks of sensing agents", vol. 5, no. 8, pp. 945-957, Aug 2006.

Appendix A - Accuracy of Methods

This appendix contains the accuracy of methods for the developed models, Simple and Corzine. The method presented uses the Maximum Likelihood estimation. The first comparison is the ML method using covariance matrix. Next, the ML Method with multiple variances for each fault for each sensor is presented. The final comparison is the fixed variance comparison. These methods are presented within different stages of the development of the method. The first is just the ML estimation. The second is testing the trigger developed and the third is using only active sensors information.

Table A.1 Accuracy of Method: Corzine Model Active Sensors with Covariance Matrix

		Accuracy (%)	
Included Faults	**Location Prediction**	*100R*	*1000R*
Outside of Normal Current	*Lines*	93.79	73.27
Outside of Normal Current	*End of Lines*	72.93	47.89
All Faults	*Lines*	55.54	43.41
All Faults	*End of Lines*	43.16	28.30

Table A.2 Accuracy of Method: Corzine Model Active Sensors with Variances

		Accuracy (%)	
Included Faults	**Location Prediction**	*100R*	*1000R*
Outside of Normal Current	*Lines*	91.31	72.13
Outside of Normal Current	*End of Lines*	72.10	46.33
All Faults	*Lines*	54.06	42.72
All Faults	*End of Lines*	42.66	27.44

Table A.3 Accuracy of Method: Corzine Model Active Sensors with Fixed Variance

		Accuracy (%)	
Included Faults	Location Prediction	*100R*	*1000R*
Outside of Normal Current	*Lines*	91.23	72.30
Outside of Normal Current	*End of Lines*	72.61	46.75
All Faults	*Lines*	54.01	42.80
All Faults	*End of Lines*	42.95	27.66

Table A.4 Accuracy of Method: Corzine Model Trigger with Covariance Matrix

		Accuracy (%)	
Included Faults	Location Prediction	*100R*	*1000R*
Outside of Normal Current	*Lines*	99.86	100.00
Outside of Normal Current	*End of Lines*	84.15	86.40
All Faults	*Lines*	59.17	59.28
All Faults	*End of Lines*	49.80	51.22

Table A.5 Accuracy of Method: Corzine Model Trigger with Variances

		Accuracy (%)	
Included Faults	Location Prediction	*100R*	*1000R*
Outside of Normal Current	*Lines*	100.00	100.00
Outside of Normal Current	*End of Lines*	78.11	74.20
All Faults	*Lines*	59.24	59.28
All Faults	*End of Lines*	46.26	43.95

Table A.6 Accuracy of Method: Corzine Model Trigger with Fixed Variance

		Accuracy (%)	
Included Faults	Location Prediction	*100R*	*1000R*
Outside of Normal Current	*Lines*	100.00	100.00
Outside of Normal Current	*End of Lines*	79.55	46.75
All Faults	*Lines*	59.24	59.28
All Faults	*End of Lines*	47.09	44.26

Table A.7 Accuracy of Method: Corzine Model All Data with Covariance Matrix

		Accuracy (%)	
Included Faults	Location Prediction	*100R*	*1000R*
Outside of Normal Current	*Lines*	99.86	100.00
Outside of Normal Current	*End of Lines*	84.15	86.40
All Faults	*Lines*	61.74	61.84
All Faults	*End of Lines*	51.13	52.44

Table A.8 Accuracy of Method: Corzine Model All Data with Variances

		Accuracy (%)	
Included Faults	Location Prediction	*100R*	*1000R*
Outside of Normal Current	*Lines*	100.00	100.00
Outside of Normal Current	*End of Lines*	78.11	74.20
All Faults	*Lines*	61.88	61.91
All Faults	*End of Lines*	47.57	45.29

Table A.9 Accuracy of Method: Corzine Model All Data with Fixed Variance

		Accuracy (%)	
Included Faults	Location Prediction	*100R*	*1000R*
Outside of Normal Current	*Lines*	100.00	100.00
Outside of Normal Current	*End of Lines*	78.11	46.75
All Faults	*Lines*	61.82	61.96
All Faults	*End of Lines*	48.38	45.63

Table A.10 Accuracy of Method: Simple Model Active Sensors with Covariance Matrix

	Accuracy (%)	
Location Prediction	*100R*	*1000R*
Lines	100.00	100.00
End of Lines	75.90	49.49

Table A.11 Accuracy of Method: Simple Model Active Sensors with Variances

	Accuracy (%)	
Location Prediction	*100R*	*1000R*
Lines	100.00	100.00
End of Lines	75.00	48.15

Table A.12 Accuracy of Method: Simple Model Active Sensors with Fixed Variance

	Accuracy (%)	
Location Prediction	*100R*	*1000R*
Lines	100.00	100.00
End of Lines	73.46	48.15

Table A.13 Accuracy of Method: Simple Model Trigger with Variances

	Accuracy (%)	
Location Prediction	*100R*	*1000R*
Lines	100.00	100.00
End of Lines	79.85	76.54

Table A.14 Accuracy of Method: Simple Model Trigger with Fixed Variance

	Accuracy (%)	
Location Prediction	*100R*	*1000R*
Lines	100.00	100.00
End of Lines	75.90	74.90

Table A.15 Accuracy of Method: Simple Model All Data with Covariance Matrix

	Accuracy (%)	
Location Prediction	*100R*	*1000R*
Lines	100.00	100.00
End of Lines	85.66	84.77

Table A.16 Accuracy of Method: Simple Model All Data with Variances

	Accuracy (%)	
Location Prediction	*100R*	*1000R*
Lines	100.00	100.00
End of Lines	79.85	76.54

Table A.17 Accuracy of Method: Simple Model All Data with Fixed Variance

	Accuracy (%)	
Location Prediction	*100R*	*1000R*
Lines	100.00	100.00
End of Lines	76.90	75.52

Table A.18 Accuracy of Method: Simple Model Trigger with Covariance Matrix

	Accuracy (%)	
Location Prediction	*100R*	*1000R*
Lines	100.00	100.00
End of Lines	85.66	84.77